Raman/LIPF data of temperature and species concentrations in swirling hydrogen jet diffusion flames: Conditional analysis and comparison to laminar flamelets☆

T.S. Cheng[a], J.-Y. Chen[b], R.W. Pitz[c],*

[a] *Department of Mechanical Engineering, Chung Hua University, Hsinchu 300, Taiwan, ROC*
[b] *Department of Mechanical Engineering, University of California Berkeley, CA 94720, USA*
[c] *Department of Mechanical Engineering, Vanderbilt University Nashville, TN 37235, USA*

ABSTRACT

Simultaneous point measurements of temperature, mixture fraction, major species (H_2, H_2O, O_2, N_2) concentrations from KrF laser-induced spontaneous Raman scattering and minor species (OH) concentrations from KrF laser-induced predissociative fluorescence (LIPF) in unswirled ($S_g = 0$), low swirl ($S_g = 0.12$), and high swirl ($S_g = 0.5$) lifted turbulent hydrogen jet diffusion flames into still air are reprocessed to obtain profiles of the Favre-averaged scalars and conditional moments. Large discrepancies between the Favre-averaged and ensemble-averaged temperature, H_2O, and OH mole fractions are found at the lifted flame region, due to density weighting of fairly large samples of unreacted mixtures. Conditional statistics are used to reveal the reaction zone structure in mixture fraction coordinates. The cross-stream dependence of conditional means of temperature and species concentration is found to be significant in the lifted flame region of the swirled flames and decreases to negligible levels with increasing streamwise position. Comparison of the measured conditional mean variation of OH vs. H_2O with a series of stretched laminar partially premixed flame and diffusion flame calculations reveals that for the unswirled flame, the differential molecular diffusion and radial dependence of conditional means are minor at $x/D = 6.4$ for stretch rates from $a = 14{,}000$ to $400\,s^{-1}$. For the low and high swirling flames, however, the measured OH vs. H_2O conditional means at the lifted flame region are not consistent with stretched laminar flame calculations. The level of partial premixing and the stretch rate decrease with increasing downstream locations. The estimated stretch rate at $x/D = 53.5$ is about 50–$10\,s^{-1}$, while at $x/D = 107$ the stretch rate is about $10\,s^{-1}$ with some measurements at adiabatic equilibrium.

© 2017 The Combustion Institute. Published by Elsevier Inc. All rights reserved.

1. Introduction

The increased global warming concerns have directed research effort towards the development of combustion devices with reduced fossil fuel consumption and low pollutant emission. For reducing the greenhouse gases, fossil fuels can be replaced with environmentally friendly, clean energy sources such as hydrogen fuel. In view of improving combustion efficiency and reducing pollutant emissions, swirling flames are considered to be one of the most effective ways to significantly increase fuel–air mixing, improve flame stability, shorten flame length, and reduce NO_x emissions [1–4] in combustion systems. Extensive studies of turbulent premixed [5–10], nonpremixed [11–17], or partially premixed [18–20] swirling flames have been reported in the literature. The non-intrusive measurements of velocity, temperature, and chemical composition from the aforementioned studies not only help reveal finite-rate chemistry effects in the swirling flames, but also provide the benchmark data set for combustion model validations. Nonetheless, the majority of previous studies have concentrated on the combustion characteristics of swirling hydrocarbon flames. Little attention has been paid to the swirling hydrogen flames. In addition, experimental studies were primarily focused on the velocity field and only a few of temperature and species concentration measurements have been made in swirling hydrogen jet diffusion flames [21–23].

With advances in computing, Mizobuchi et al. [24,25] and Yoo et al. [26] used three-dimensional direct numerical simulation (DNS) to study the flame stabilization and structure in nonswirling lifted turbulent hydrogen jet flames. The DNS results by Yoo et al. [26] give the structure of a turbulent lifted hydrogen jet flame in remarkable detail but the computation cost

(3.5 million CPU hours taking 15 days on 10,000 cores) of such calculations limit their widespread application. Combustion modeling with more modest resources and faster turnaround is desired for design applications. Klimenko [27] and Bilger [28] separately developed the conditional moment closure (CMC) model that can predict accurately the liftoff height and radial profiles of scalars in hydrogen jet flames [29–32]. Moreover, the first-order CMC model was also applied to study autoignition of a turbulent methane jet [33], extinction and re-ignition events in turbulent non-premixed hydrocarbon combustion [34], soot formation in turbulent, non-premixed ethylene flames [35], autoignition of methane-based fuel blends [36], and combustion in homogeneous charge compression ignition (HCCI) conditions [37]. Using the second-order CMC model, turbulent methane/air piloted jet diffusion flames [38], a turbulent $CH_4/H_2/N_2$ jet diffusion flame [39], and a lifted hydrogen jet flame [40] were investigated. Additionally, a 3D elliptic CMC model was used to study a low-swirl-stabilized nonpremixed methane flame [41]. Recently, the Large Eddy Simulation (LES)/3D-CMC model with detailed chemistry was employed to simulate a swirl-stabilized non-premixed methane flame with local extinction [42].

The above numerical studies have shown that the CMC models yield satisfactory solutions with most of the models using cross-stream averaging. Radial independence of conditional means is a convenient assumption of the CMC model as applied to jet flames.

The assumption of radial independence of conditional scalars has been examined experimentally in jet flames. In H_2 jet flames, radial dependence of conditional scalars is found near the flame base but radial dependence is negligible in the upper part of the flame [43,44]. In piloted jet diffusion flames of methanol and N_2-diluted propane jet flames, no radial dependence of conditional scalars is found at 20–25 diameters from the jet exit [28]. In piloted air-diluted methane jets, the conditional scalars show significant radial dependence near the flame base that diminishes to negligible dependence beyond 45 diameters from the jet exit [45]. However, the assumption of radial independence of conditional means has not been examined in swirling jet flames.

In the present work, we check the assumption of radial independence of the conditional means in swirling lifted hydrogen jet diffusion flames by determining to what extent the conditional means of temperature and species concentrations vary with radius. Many combustion models use Favre-averaging and the previous report [46] presented time-averaged mean profiles of temperature and species concentration. In this paper, we present the Favre-averaged profiles of mixture fraction, temperature, and species mole fractions in the swirling lifted hydrogen jet flames to reveal turbulence-chemistry effects. To test the assumption of laminar flamelets used in many combustion models, we compare the measured conditional means of OH vs. H_2O to calculated libraries of stretched laminar diffusion flames and stretched partially premixed flames in various regions of the swirled lifted jet diffusion flames. This comparison tests whether the OH vs. H_2O variation in the turbulent flame can be predicted by these flamelet libraries and allows us to estimate the strain rates in the turbulent swirling lifted flames.

2. Experimental methods

2.1. Swirl burner

The schematic diagram of the swirl burner is shown in Fig. 1. The fuel exits the nozzle into still atmospheric air. The swirled combustor is operated with fuel either axially and/or tangentially supplied to the combustor with each of these flows being controlled separately. It should be noted that the swirling mechanism of the present burner (fuel swirling) is totally different from that
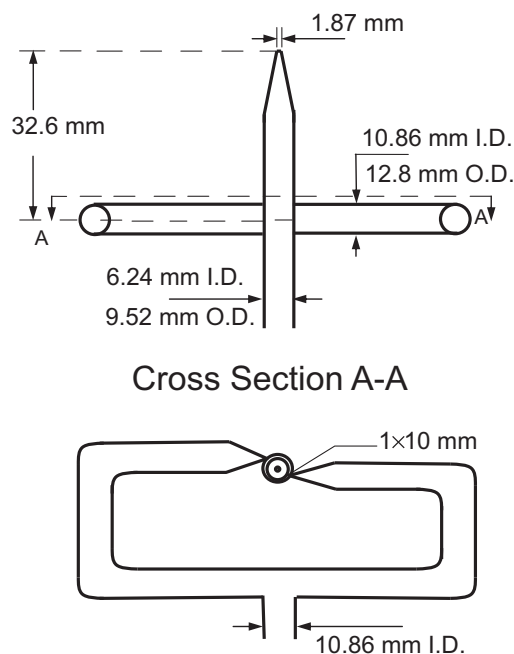

Fig. 1. Schematic diagram of the swirl burner.

of the traditional swirl burners (air swirling). The vertical straight tube has a 6.24-mm inner diameter with conical nozzle (5° taper) to an exit diameter of 1.87-mm. The wall thickness at the exit of the jet nozzle is 0.2 mm to minimize wake effects. The jet Reynolds number is 12,500 based upon nozzle exit diameter ($D = 1.87$ mm) and a jet exit velocity of 660 m/s with hydrogen fuel. For these conditions, three flow regimes are investigated: 1) an axial jet flame ($\dot{m}_{axial} = 0.157$ g/s, $S_g = 0$), 2) a mixed jet flame ($\dot{m}_{axial} = 0.079$ g/s $\dot{m}_{tangential} = = 0.079$ g/s, $S_g = 0.12$), and 3) a tangential jet flame ($\dot{m}_{tangential} = 0.157$ g/s, $S_g = 0.5$), where S_g is the geometric swirl number and $\dot{m}$ is the mass flowrate of H_2 fuel. The geometric swirl number is defined as [47]:

$$S_g \frac{\pi r_e r_o}{A_t} \left(\frac{\dot{m}_{tan}}{\dot{m}_{tot}} \right)^2 \tag{1}$$

where r_e is the jet exit radius, r_o is the radius of the tangential inlets from the jet centerline, A_t is the total area of the tangential inlets, $\dot{m}_{tan}$ is the tangential mass flowrate, and $\dot{m}_{tot}$ is total mass flowrate. The swirled H_2 jet flame is similar to one studied by Yuasa [48]. Swirl is added by two slot injectors (1 mm × 10 mm) that inject fuel tangent to the inner diameter of the straight fuel tube (see Fig. 1). For the flames, the jet exit Mach number is 0.52 and compressibility effects on temperature are not important (< 20 K for the initial fuel temperature of 295 K). All three flames have a visual liftoff height of approximately 6 diameters.

2.2. UV Raman/LIPF system

The schematic diagram of the UV Raman/LIPF system is shown in Fig. 2. Details on the Raman scattering/LIPF measurement for turbulent flames and its calibration have been provided earlier [46,49]. Spontaneous vibrational Raman scattering and OH laser fluorescence are induced by a tunable narrowband KrF excimer laser (248 nm, 20 ns pulse) to simultaneously measure major species concentrations (N_2, O_2, H_2O, and H_2), OH concentration, and temperature. The pulse energy of the KrF laser is ~150 mJ with 95% of the pulse energy is in the narrowband mode (0.001 nm linewidth) while 5% of the pulse energy is in the broadband mode (~1 nm linewidth). The KrF narrowband laser is tuned to